Thermochemical Property Measurements of FLiNaK and FLiBe in FY 2020

Chemical and Fuel Cycle Technologies Division

Thermochemical Property Measurements of FLiNaK and FLiBe in FY 2020

by
T. Lichtenstein, M.A. Rose, J. Krueger, E. Wu, and M.A. Williamson
Chemical and Fuel Cycle Technologies Division, Argonne National Laboratory

November 17, 2020

CONTENTS

1.   Introduction

The technical bases and methods developed at Argonne to measure thermochemical properties of molten salt mixtures are summarized and results provided to show the precision achieved. These methods include measurements of phase transition temperatures and heat capacity at temperatures to approximately 700 °C for eutectic mixture of 46.5-11.5-42.0 mol% LiF-NaF-KF (FLiNAK) and 67-33 mol% $LiF-BeF_2$ (FLiBe). Details of procedures, calibrations and operation of instruments are discussed and results are compared with values available in the literature. Additional discussions address the sources of error and estimated uncertainties in the reported values.

2.   Source Materials and Salt Preparation

Reagents used to prepare salt mixtures for measurements were purchased at the highest purities available (better than 99.9% by trace metals analysis). Appendix A provides material certificates for representative salt reagents provided by the manufacturers.

Salt mixtures and samples to be analyzed were prepared in argon atmosphere gloveboxes in which oxygen and moisture levels are both maintained at below 10 ppm. Reagent salts were characterized by using powder X-ray diffraction prior to use to confirm the compositions and determine if significant amounts of impurities were present. Samples were fixed onto slides with double-sided tape and sealed with Kapton polymer film while inside the glovebox to avoid contamination throughout the analysis. A Bruker D5000 X-ray diffraction (XRD) system was used to measure the pattern over the range $2\theta = 10°$ to $100°$. Figure 1 shows the XRD diffraction patterns measured for the reagent LiF, KF, and NaF. The circles indicate the intensities and locations of peaks listed in the International Center for Diffraction Data database that were used to confirm the identities of the reagent salts.

Beryllium fluoride was purchased as industrial grade material from Materion. The salt particles had an abundance of visible dark-colored inclusions thought to be graphite; a representative grain is shown in Figure 2. Steps were taken to purify the material before producing salt mixtures for analysis. The first step of purification was to manually remove visible pieces of graphite from the material. The salt was then heated at 300 °C to remove adsorbed water. The BeF_2 salt was then melted and held at 700 °C to allow minute pieces of solid impurities to either settle to the bottom or rise to the top of the molten salt. After cooling to solidify, the top and bottom sections of the salt block were removed and discarded. The relatively pure middle portion was ground and the process repeated several times until there was no visible color change in the salt from top to bottom and no impurities were observed. Three samples of BeF_2 purified in this manner were analyzed for total dissolved oxygen using a LECO 836 Oxygen/Nitrogen Analyzer.

(a)

(b)

(c)
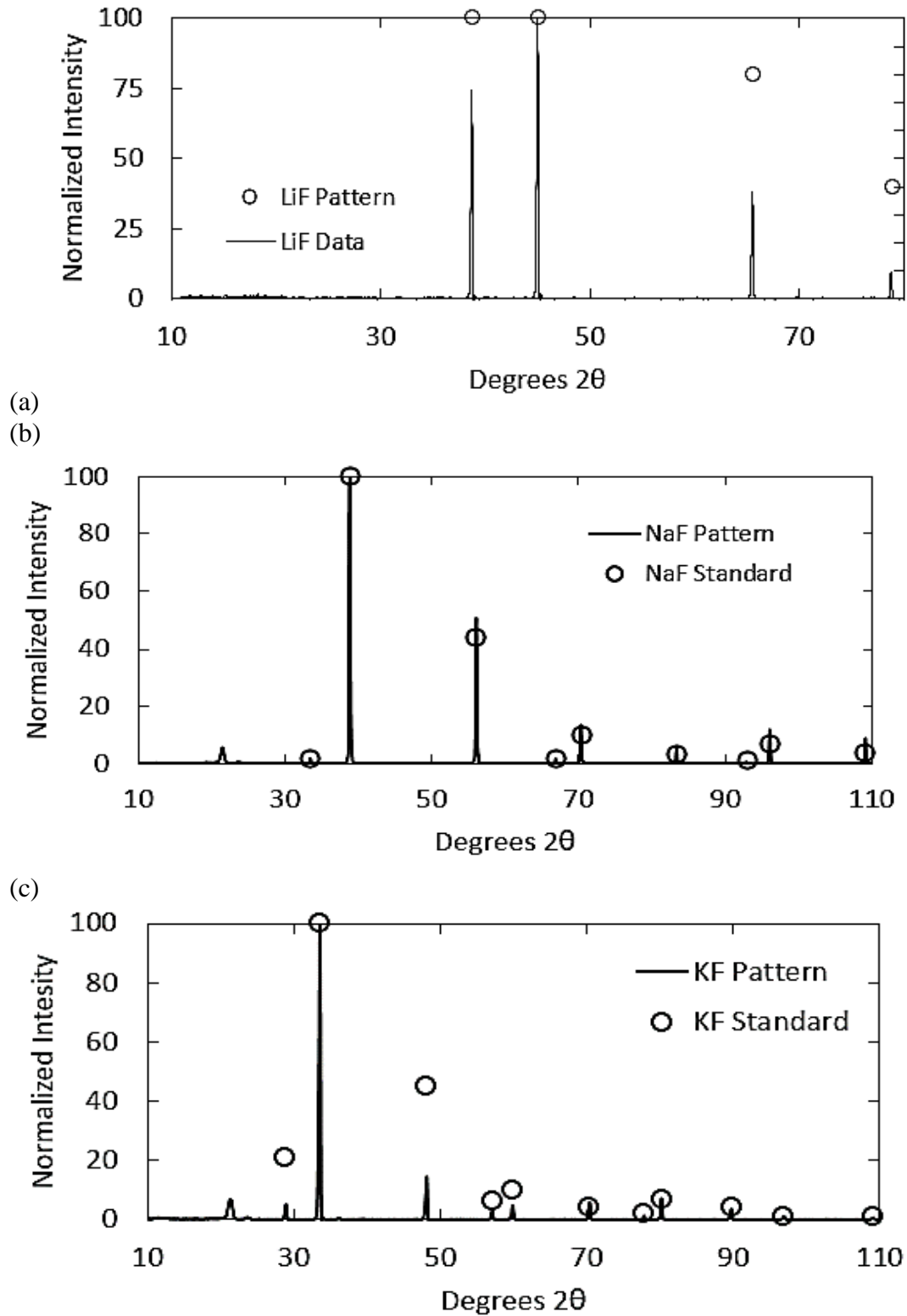
Figure 1: Measured X-ray Diffraction Patterns and Peak Intensity compared with Literature Data for Reagent Salts (a) LiF, (b) NaF, and (c) KF
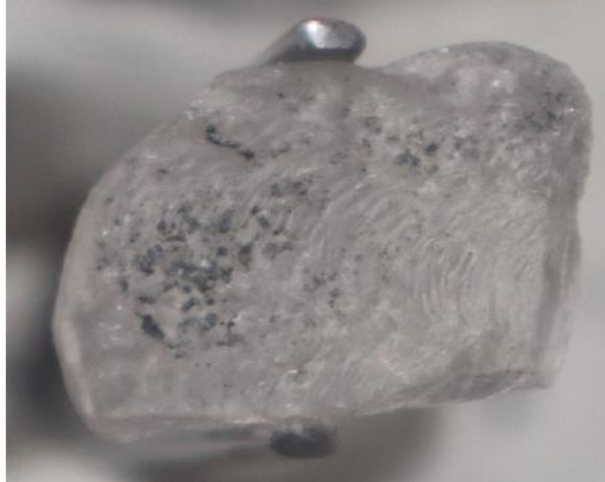
Figure 2. Photograph of As-Received BeF_2 Salt Granule

Table 1 shows the results of that analysis; the results are accurate within 25% of the reported values. The measured oxygen content includes that in oxides and water impurities.

Table 1. Results of Oxygen Analysis of BeF_2 Samples

Sample #	Oxygen (wt %)
1	1.2
2	1.3
3	1.2

Salt mixtures were prepared by placing the appropriate amounts of reagent salts in a nickel crucible and heating twice in a furnace to melt and homogenize the material. The as-batched compositions of the two mixtures are shown in Table 2. The nickel crucible was manually polished with steel wool and rinsed with methanol to remove any oxide residue and prevent oxide contamination of the mixtures. The fused salt was removed from the crucible and ground to a fine powder after each heating by using a mortar and pestle.

Table 2: As-batched Compositions of FLiNaK and FLiBe Salts

FLiNaK (g)[*]			FLiBe (g)	
LiF	NaF	KF	LiF	BeF_2
2872.15	1123.43	5773.59	524.3463	468.0840

*Based on [1].

Wet analytical methods were used to analyze the elemental compositions of salt batches used for each property measurement. Replicate samples were dissolved in nitric acid and analyzed by inductively coupled plasma-optical emission spectroscopy (ICP-OES) using a Perkin Elmer Optima Model 8300DV ICP-OES. Analyses were performed to determine the homogeneity of the mixture and the results are collected in Table 3 for major elements of FLiNaK represented as the constituent fluorites.

Table 3: Major Elemental Analysis of FLiNaK by ICP-OES (mol %) [1]

	LiF	NaF	KF
Sample 1	47.0	11.6	41.4
Sample 2	46.3	11.6	42.1
Sample 3	46.1	11.3	42.6
Average	46.5	11.5	42.0
1 s	0.5	0.2	0.6

Aliquots of the solutions used for ICP-OES analyses were further diluted and used to measure the amounts of trace contaminants in each FLiNaK salt sample by using inductively coupled plasma-mass spectrometry (ICP-MS); those results are shown in Table 4. The ICP-MS technique is typically accurate to ±10%. The levels of Mg, Cr, Mn, Fe, Rb, and Cs measured in the salt are consistent with the contamination levels measured in the reagents. However, the concentrations of Ni and Ca measured in the salt were significantly higher than the concentrations measured in any of the reagents. Contamination of the salt with Ni may have come from the nickel crucible used for melting the salt and the nickel impeller used to stir the molten salt. The calcium contamination was likely introduced after production when the salt was ground using a large ceramic mortar and pestle.

Table 4: Trace Element Analysis of FLiNaK by ICP-MS (ppm) [1]

	Mg	Ca	Cr	Mn	Fe	Ni	Rb	Cs
Sample 1	< 82	1490	< 11	< 4	< 200	115	31.9	2.3
Sample 2	< 30	944	< 8	< 2	< 140	137	25.8	1.8
Sample 3	< 25	510	< 7	< 3	< 120	118	26.3	1.4
Average		981				123	28.0	1.8
1 s		490				12	3.4	0.4

< values give detection limits.

Analysis of the mixture of FLiBe made for property measurements is in-progress.

3.   Thermal Analysis by Differential Scanning Calorimetry

Differential scanning calorimetry (DSC) is used to perform thermal analysis of salt systems and measure the heat capacity. Hermetically sealed gold sample crucibles (TA Instruments, Wood Dale, IL) are used to contain salts for analysis, as pictured in Figure 3. The gold cells are cleaned before use by washing first with water, then with concentrated hydrochloric acid, and then again with water. The cells are allowed to air dry before being placed in the air lock of the glovebox, which is then evacuated using a mechanical pump for 30-60 minutes before the cells are moved into the glovebox. The gold cells are carefully weighed then loaded with crushed salt and sealed twice by using a mechanical sealer. This procedure ensures that the salt samples are not exposed to an atmosphere with greater than 10 ppm oxygen and 1 ppm water, which are the upper limit values maintained in the glovebox, either prior to or during DSC analyses.
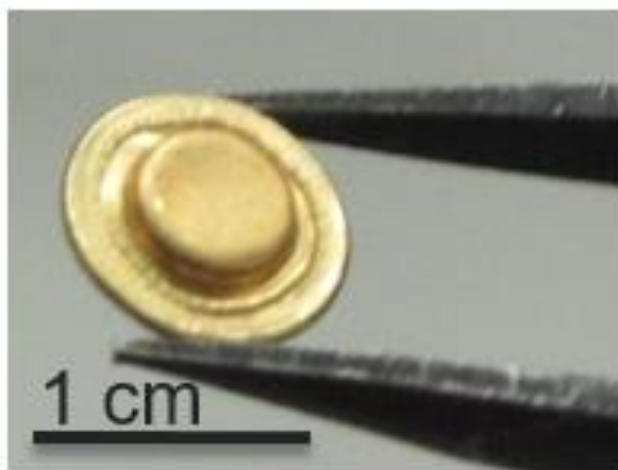
Figure 3: Hermetically Sealed Gold Sample Crucible Showing Sealed Side

Thermal properties of the salt samples are measured by using a Netzsch (Model STA Jupiter 449C) standard thermal analyzer (STA) with thermogravimetric analysis (TGA). The STA is operated inside of an argon atmosphere glovebox maintained at less than 10 ppm oxygen and less than 1 ppm water. A continuous high purity argon purge inside of the instrument is used to provide an atmosphere surrounding the sample with even lower oxygen and moisture conditions during measurements. Prior to the heat capacity measurements, each sealed crucible containing a salt sample is heated to a temperature above the melting point of the sample to ensure the material is well mixed and the crucible is well sealed. The sample is subsequently heated twice at 5 °C min^{-1} using the heating profile shown in Figure 4 to measure the melting point and detect other phase transitions. Two sequential analyses are run to verify system stability.
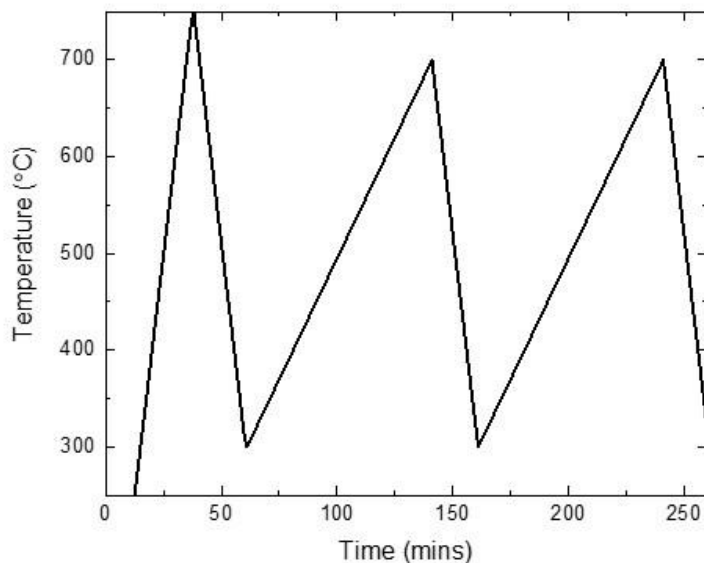
Figure 4. Heating Profile to Determine Phase Transition Reactions.

3.1   Temperature Calibration of DSC

The temperatures measured by the DSC are calibrated before use by measuring the melting points of five pure metal standards from Netzsch (Sn, Zn, Al, Ag, and Au) having known values that span the range from 231.9 to 1064.2 °C. The melting point of each metal standard is measured twice at the same heating rate of 5 °C min^{-1} used to analyze the salt samples and by the same method. A representative thermogram measured for a Zn standard is shown in Figure 5. The melting point is determined from the onset temperature, labelled T_{onset}, which is the temperature at which the
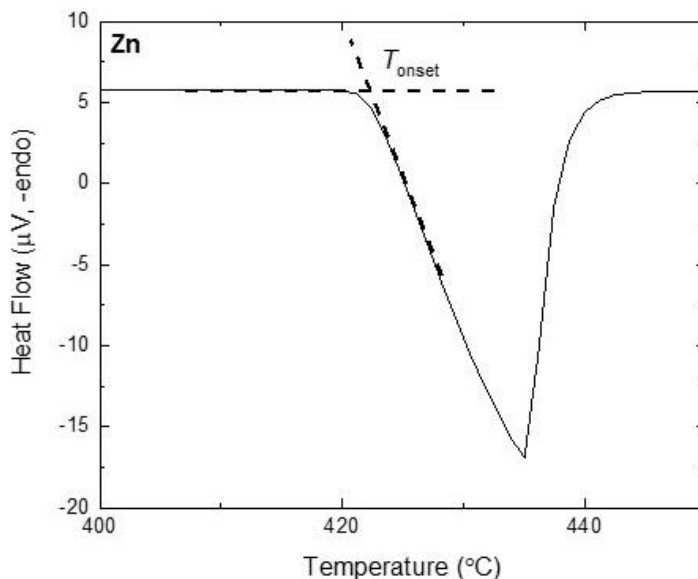
Figure 5. Determination of the Transition Temperature by Onset Extrapolation for Pure Zn.

extrapolated baseline meets the linear extrapolation from the inflection point of the heating curve (illustrated by the dashed lines in Figure 5). This is done automatically by the software used to run the scan.

The repeatability is typically excellent for duplicate measurements made with each metal standard, but the measured melting temperatures usually differ slightly from the reference values used by the software due to uncontrollable variables. Figure 6 shows the results of duplicate calibration measurements made prior to salt measurements expressed as Delta T = T(measured)-T(reported). Duplicate measurements for Sn, Ag, and Au overlap but small differences are seen for Zn and Al. A quadratic regression is used by the Netzsch Proteus software to calibrate the measured temperatures over the full range using the reported values for the metal standards. The difference between the values of the calibration curve at the melting temperature of each standard metal and the measured value represents the accuracy of measurements made at and near that temperature.
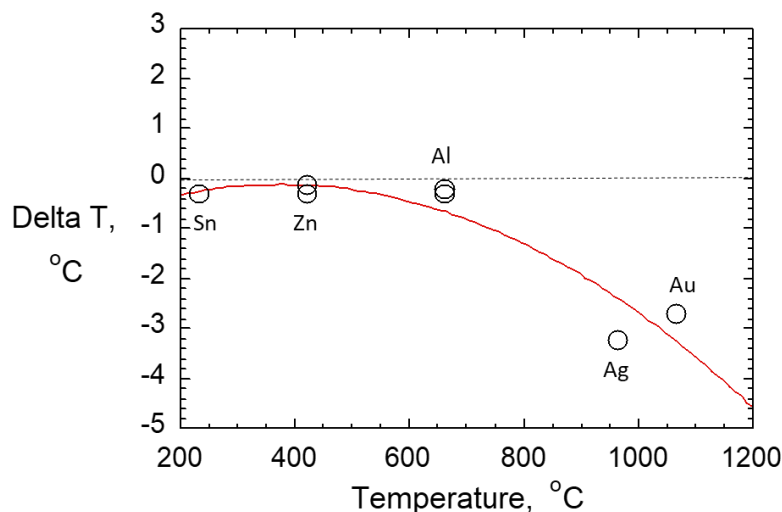
Figure 6: Calibration curve for duplicate measurements of metal standards prior to DSC analyses of salts

All calibration results are being tracked to detect significant changes in performance and long-term bias of the DSC. A summary of the mean calibration metal melting temperatures are shown in Table 5 along with values for two standard deviations (2s), which quantify the precision of measurements at each temperature. Calibrations made at different times resulted in slightly different calibrations curves due to environmental effects, but the accuracies were always within about 1 °C for temperatures below 700 °C and 2 °C for temperatures above 700 °C. These differences are taken into account by using the calibration curve. No bias has been observed through about 2.5 years of operation and the deviations between reported and measured melting

temperature remain within 2 °C for temperatures up to 660 °C and within about 4 °C at higher temperatures.

Table 5: Mean Melting Temperatures for Calibration Metals Measured by DSC over 2.5 Years

Calibration Metal	Sn	Zn	Al	Ag	Au
Reported Melting T, °C	231.9	419.6	660.3	961.8	1064.2
Mean Measured Melting T, °C	231.0	419.8	660.8	959.3	1062.4
2 s, °C	0.8	2.0	0.9	2.2	3.8

3.2 Thermal Analysis of FLiNaK Salt

Three portions of the FLiNaK salt (21.11 mg, 24.57 mg, and 24.64 mg) were hermetically sealed in gold cells under an inert atmosphere for thermal analysis. Figure 7 shows the signals from the heating cycles of duplicate DSC scans of each sample run at 5 °C min^{-1} on the same plot, with solid and dashed lines representing the first and second runs, respectively. The repeatability observed in the replicate scans indicates the system remained stable during the analyses. The small differences in the shapes of the scans of the three samples are due to minor differences in the environment on the days the scans were made. No peaks other than the eutectic melting peak are seen, although a small shoulder is noticeable at approximately 465 °C in some scans.
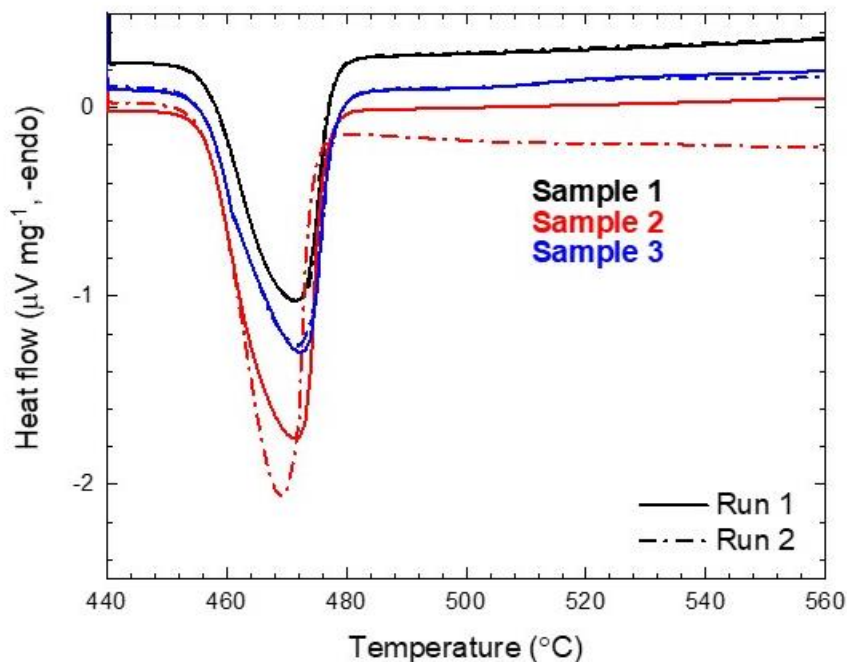

Figure 7: DSC Scans of FLiNaK Salt Samples at 5 °C min^{-1} Scan Rate

The Netzsch software Proteus was used to determine the onset temperature of the eutectic peak in each scan and the results are listed in Table 6. The average of the measured melting onset temperatures was 456.2 °C and the standard deviation was 0.6 °C. The instrument was calibrated

Table 6: Measured Onset Temperatures for Eutectic FLiNaK

Sample	Run	Onset Temperature (°C)
1	1	455.8
	2	456.1
2	1	456.5
	2	456.9
3	1	456.5
	2	455.2
Average		456.2
1 s		0.6

prior to use and the precision of DSC measurements has been determined to be ±1 °C up to 700 °C based on replicate calibrations with five different metallic standards. The same method was used to determine the onset melting temperatures of the standards during calibration runs and analyses of the salt samples. The variations in the measured onset melting temperatures of the three samples listed in Table 6 are within the instrumental uncertainty.

To verify the stability of liquid FLiNaK heat flows, a sample was subjected to 11 cycles of heating-cooling through the melting temperature, shown in Figure 8. The heat flow of the liquid was unchanged and the onset of the eutectic was stable across cycles to within 0.3 °C, which is well within the accuracy of the calibration and indicates that the composition of the FLiNaK sample and thermal contact with the crucible remained stable.
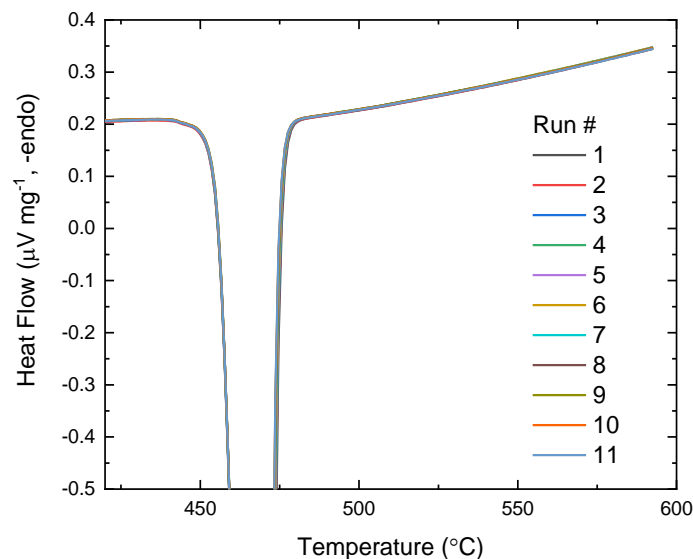
Figure 8: Eleven Consecutive Heating-Cooling Cycles on a FLiNaK Sample

3.3   Thermal Analysis of FLiBe Salt

Three portions of the FLiBe salt (21.82 mg, 21.83 mg, and 21.73 mg) were prepared for thermal analysis in the same manner as described for FLiNaK in Section 3.2. Figure 9 shows the signals from the heating cycles of duplicate DSC scans with each sample run at 5 °C min^{-1} on the same plot. The repeatability of the replicate scans indicates the FLiBe salt remained stable during the analyses. The small differences in the shapes of the DSC scans with the three samples are due to minor differences in the environment on the three days the scans were made. Two peaks are seen in each scan. The smaller peak at ~416 °C labelled Reaction 1 in Figure 9 corresponds to the eutectic transition reaction where the two-phase solid of BeF_2 and Li_2BeF_4 melts. The larger peak that occurs at ~452 °C and is labelled Reaction 2 corresponds to the congruent melting of Li_2BeF_4. The transition temperatures measured in the thermal analyses are collected in Table 7.
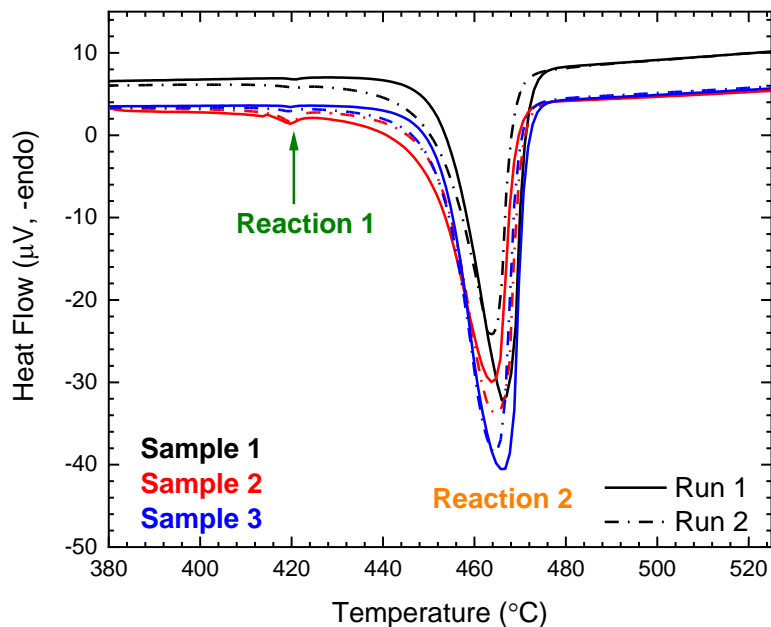
Figure 9: DSC Scans of FLiBe Salt Samples

The high temperature Reaction 2 is measured to occur close to the literature value of 459 °C [2] but the low temperature Reaction 1 occurs about 53 °C higher than the literature value of 363 °C [3]. The thermal analysis reported in literature was based on heating and cooling curves at 1–2 °C min^{-1} but the scan rate used to identify the eutectic at 363 °C was not indicated, so undercooling during the cooling scan may have resulted in the reported value being too low. To verify no additional reactions occurred in our analyses, a scan was performed over an expanded temperature range and both the heating and cooling curves are shown in Figure 10. The heating

Table 7: Measured Transition Temperatures for FLiBe

Sample	Run	Transition Temperature (°C)	
		Reaction 1	Reaction 2
1	1	418.6	453.2
	2	416.9	452.5
2	1	416.6	452.3
	2	413.9	450.2
3	1	417.6	452.4
	2	415.9	452.0
Average		416.6	452.1
1 s		1.5	0.9
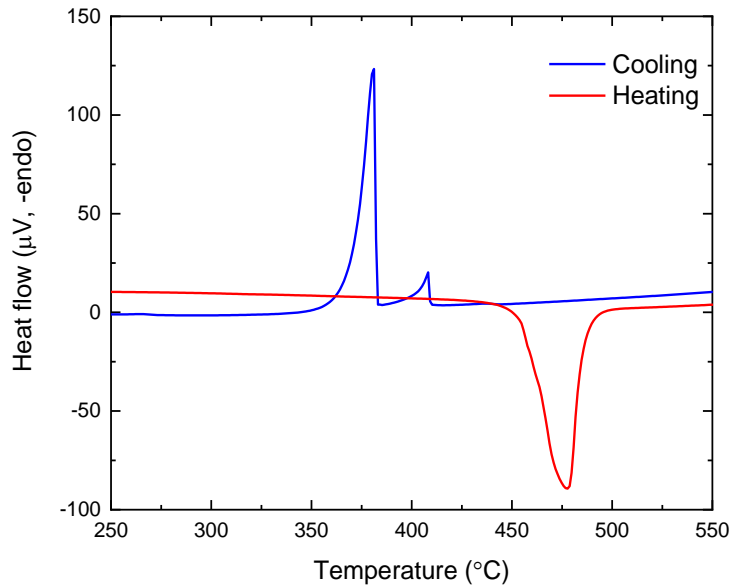
Figure 10: Expanded Temperature Range Heating-Cooling DSC Scan for FLiBe

curve has no features at temperatures below 380 °C, leading to the conclusion that the feature observed at 416°C is most likely due to the eutectic transition reaction. This is confirmed by the two peaks seen in the cooling curve that reflect the reverse of the two transition reactions observed in the heating curve. Undercooling of 30–50 °C is also observed in the comparison, with the small peak occurring at 408 °C signaling the start of solidification and the large peak occurring at 381 °C being associated with the completion of solidification. This result indicates the value of 363 °C reported in the literature [3] is probably affected by supercooling and the value of 416.6 °C is more accurate.

4. Heat Capacity Measurements

4.1 Heat Capacity Measurement Method

The heat capacity measurements follow a standard three-step procedure adapted from that described in ASTM E1269 [4]. This includes separate measurements with two empty crucibles, with a sapphire reference and an empty crucible, and with a salt sample and an empty crucible. The procedure employed at Argonne uses gold crucibles that are weight-matched to within 1.5% for all measurements. The sapphire reference and salt samples sealed within the gold crucibles are weight matched to within 1%. The three measurements are made following the thermal profile illustrated in Figure 11 for measurements with FLiBe: a 15-minute isothermal hold to measure the heat flow, a linear ramp at 10 °C min^{-1} to 730 °C, then a 15-minute isothermal hold to measure the heat flow at 730 °C. A similar profile was used for measurements of FLiNaK except the low temperature isothermal hold was at 420 °C.
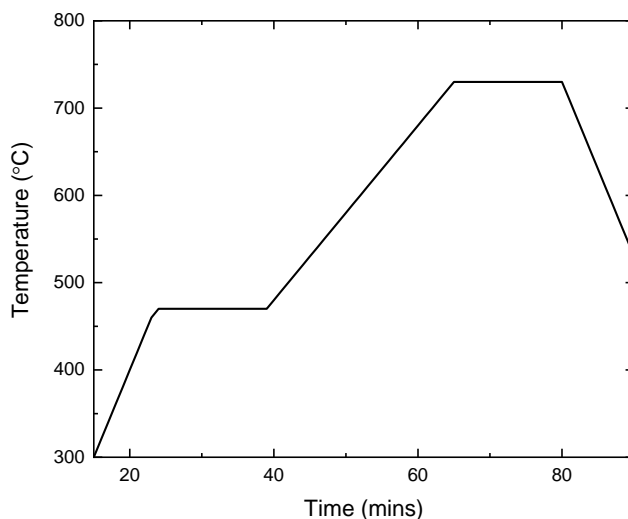
Figure 11. Heating Profile for Heat Capacity Measurements of FLiBe.

An instrumental baseline using two empty, weight-matched crucibles is run first to determine the instrument bias. One of the empty crucibles is replaced with a crucible containing a sapphire standard and run in the same thermal profile, then the sapphire crucible is replaced with a crucible containing a salt sample and run using the same thermal profile. Heat flows through the sapphire and salt sample are corrected for the instrumental bias by subtracting the heat flow of the instrument baseline determined in the first step with empty crucibles. The baseline correction is done automatically by the Netzsch Proteus software.

In the Argonne procedure, the heat flows measured at each temperature are also corrected for material-related effects by using differences in the heat flows measured during isothermal holds

before and after the linear ramp. A linear baseline is interpolated between those measured values to represent temperature-dependent material effects. Values of the interpolated baseline are calculated as a function of time during the temperature ramp by using Equation 1.

$$\varphi_{iso}(t) = \varphi_{iso,st} + \frac{\varphi_{iso,end} - \varphi_{iso,st}}{t_{end} - t_{st}}(t - t_{st}) \tag{1}$$

where $\varphi_{iso,st}$ is the heat flow measured at the end of the low temperature hold, $\varphi_{iso,end}$ is the heat flow measured at the end of the high temperature hold, t_{st} is the time at the start of the heating ramp, and t_{end} is the time at the end of the ramp. The corrected heat flow, $\varphi_{corr}(t)$, at each point during the ramp is calculated by subtracting the interpolated baseline, $\varphi_{iso}(t)$, from the experimental heat flow, $\varphi_{exp}(t)$, as indicated in Equation 2. The method is visualized in Figure 12.

$$\varphi_{corr}(t) = \varphi_{exp}(t) - \varphi_{iso}(t) \tag{2}$$
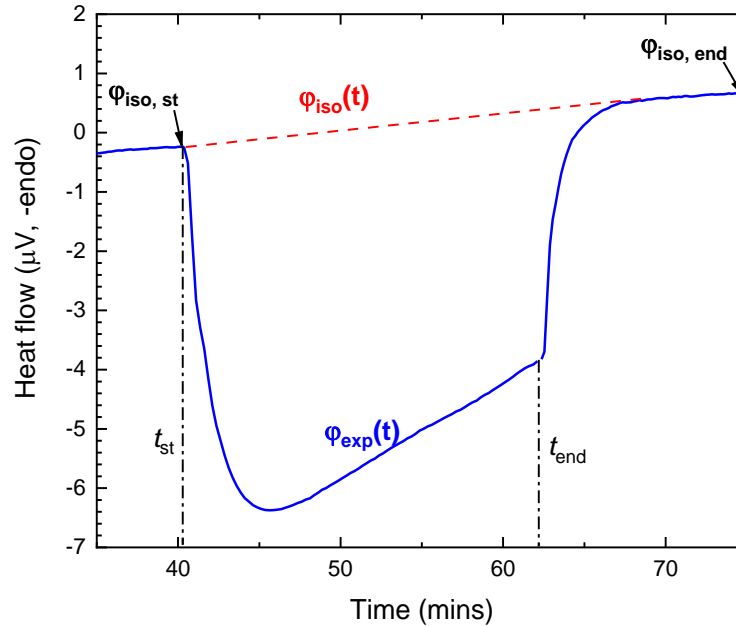
Figure 12. Visual Representation of the Correction of Heat Flow using Isotherms

Differences in the heat flows measured during isotherms at 420 or 470 °C and at 730 °C can be caused by material properties, thermal contacts, and small changes in environmental conditions during the DSC measurement. Data from experiments where the DSC signals of the two isothermal holds differ by more than 2 µV are considered to indicate system instability and the results are discarded.

The heat capacity of the sample, C_p^s, is calculated relative to the heat flows measured for the sample and reference material scaled by the material and crucible masses by:

$$C_\mathrm{p}^s = \frac{m_r}{m_s}\frac{\Delta\varphi_{corr,s}}{\Delta\varphi_{corr,r}}C_p^r + \frac{m_{cr}^r - m_{cr}^s}{m_s}C_p^{cr} \tag{3}$$

where m_s and m_r are the masses of the sample and sapphire; m_{cr}^s and m_{cr}^r are the masses of the crucibles containing the sample and sapphire; $\Delta\varphi_{corr,s}$ and $\Delta\varphi_{corr,r}$ are the heat flows of the sample and sapphire, both corrected for the baseline and isothermal drifts; and $C_\mathrm{p}^s, C_\mathrm{p}^r$, and C_p^{scr} are the heat capacities of the sample, sapphire, and crucible, respectively.

4.2   Heat Capacity of FLiNaK Salt

Three samples of the FLiNaK salt (referred to as S1, S2, and S3) were prepared for heat capacity measurements. The sample and sapphire masses for the three measurements are given in Table 8.

Table 8: Samples and Sapphire Used for FLiNaK Heat Capacity Measurements

Sample	Sapphire	FLiNaK		
		S1	S2	S3
Samples mass (mg)	21.82	22.08	22.01	21.88
Crucible mass (mg)	372.39	374.53	373.64	371.38

The measurements were run and signals corrected using the procedure described in Section 4.1. The corrected DSC signals were used to calculate the heat capacity of FLiNaK salt by using Equation 3. Figure 13 shows the calculated heat capacity values for FLiNaK samples S2 and S3
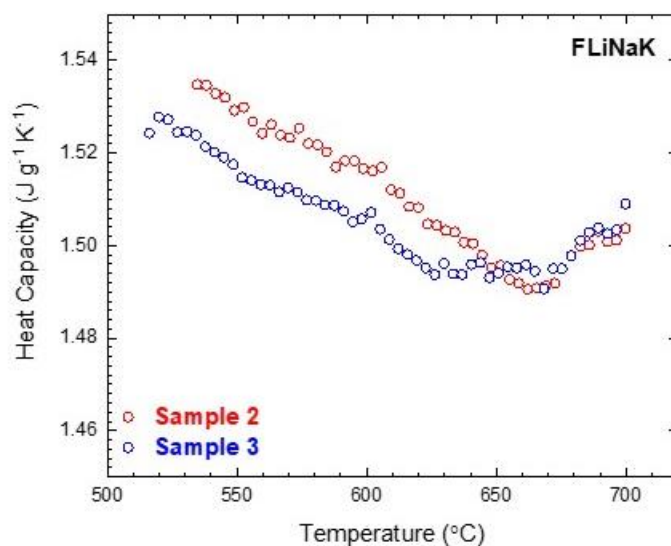

Figure 13. Calculated Heat Capacity of FLiNaK For Samples S2 and S3

plotted as a function of temperature in for liquid-state FLiNaK and values at selected temperatures are tabulated in Table 9. The heat capacity measurement for sample S1 is still in-progress.

Table 9. Average Heat Capacity at Select Temperatures for FLiNaK Salt

Temperature (°C)	Heat Capacity (J g^{-1} K^{-1})	
	S2	S3
600	1.517	1.507
625	1.504	1.493
650	1.496	1.494
675	1.492	1.495
700	1.504_	1.509

In general, the heat capacity decreased about 0.05 J g^{-1} K^{-1} in both samples over the temperature range of 515–640 °C before increasing slightly by 0.01 J g^{-1} K^{-1} from 640–700 °C. The observed decrease in heat capacity with temperature is unexpected. Heat capacity for a liquid is generally expected to be constant or increase with temperature. The decreasing heat capacity trend may be due to the eutectic phase transition occurring during the measurement. This is seen in Figure 14 between 440 and 520°C for FLiNaK. The average of the measured heat capacity of FLiNaK ranges from about 1.52 to 1.49 J g^{-1} K^{-1} over the temperature range of 520–700 °C with a maximum difference of 2% of the mean value for two measurements.
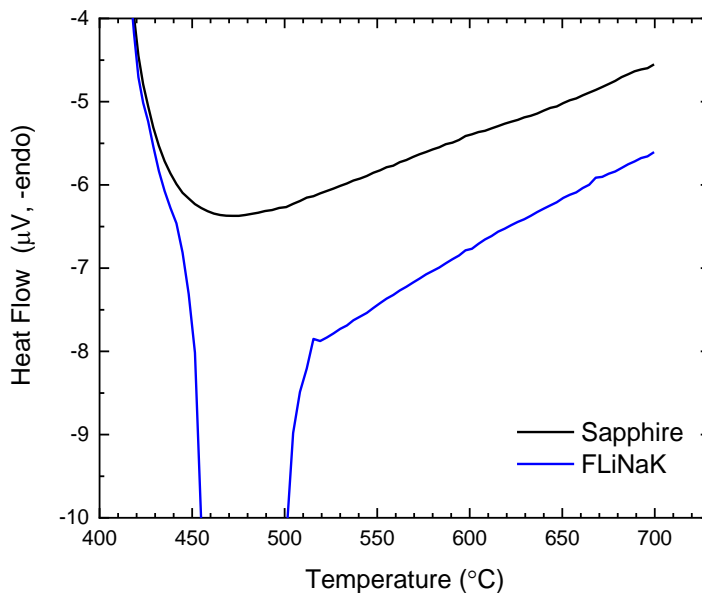

Figure 14. Baseline and Isothermal-Corrected Signals for DSC with Sapphire and FLiNaK

4.3   Heat Capacity of FLiBe Salt

The heat capacity of FLiBe was measured using the same samples that had been used for thermal analysis. The sample and crucible masses are given in Table 10**.** Measurements with sample 3 (S3) are in progress**.** The measurements for heat capacity were made as described in Section 4.1. The calculated heat capacity for FLiBe is shown graphically in Figure 15 and values at selected temperatures are given in Table 11.

Table 10: Samples and Sapphire Used for FLiBe Heat Capacity Measurements

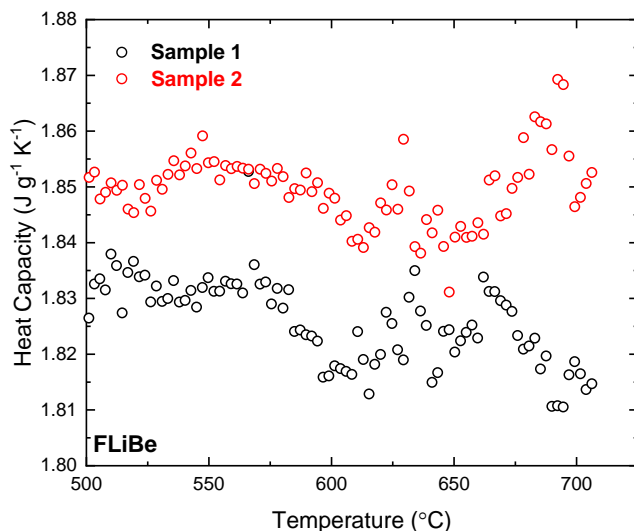| Sample	Sapphire	FLiBe		
		S1	S2	S3
Samples mass (mg)	21.82	21.82	21.83	21.73
Crucible mass (mg)	372.39	368.26	369.33	368.75

Figure 15. Calculated Heat Capacity for FLiBe Samples 1 and 2 (S1, S2).

Table 11. Calculated Heat Capacity at Select Temperatures for FLiBe Salt

Temperature (°C)	Heat Capacity (J g^{-1} K^{-1})	
	S1	S2
600	1.82	1.85
625	1.83	1.85
650	1.82	1.84
675	1.82	1.85
700	1.82	1.85

Baseline and isothermal corrected data for heat capacity measurements of FLiBe are shown in Figure 16. The smooth transition from the increasingly negative values at low temperatures to linearly increasing heat flow suggests both the sapphire and FLiBe do not undergo a phase transition between 500 and 700 °C.
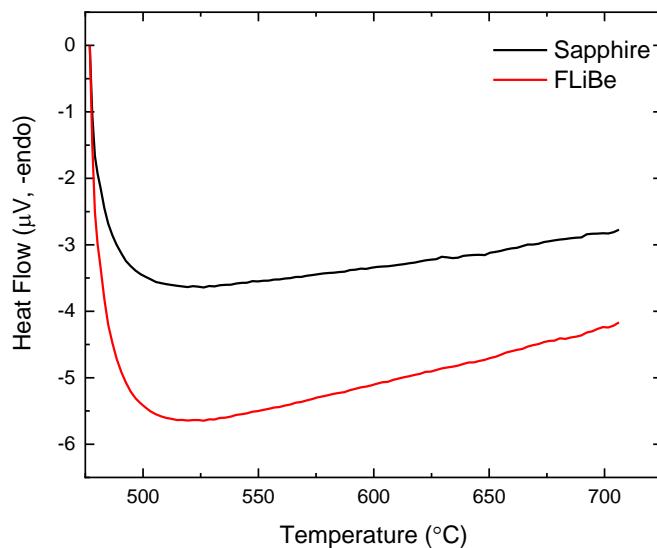

Figure 16. Baseline and Isothermal-Corrected DSC Signals for Sapphire and FLiBe

The calculated heat capacity does not show the same trend with temperature observed for FLiNaK, most likely due to complete melting of the sample during the low temperature isothermal hold, since no discontinuity in the shape of the heat flow is seen in Figure 16. However, there is more scatter in the calculated heat capacity of the FLiBe samples at temperatures above 600 °C than at lower temperatures, suggesting FLiBe may be volatilizing within the sealed cell and reducing its contact with the gold crucible. The calculated average heat capacity is about 1.84 J g^{-1}K^{-1} and constant between 500 and 700 °C with a maximum difference of 5% of the mean value.

5. Discussion

These measurements have been repeatable with a deviation of 5% of the average values reported for FLiBe and 2% for FLiNaK. These deviations are consistent with the uncertainty expected for heat capacity measurements by DSC [5]. Major factors affecting the precision include weight matching the samples and crucibles to the sapphire standard, placement of the samples within the DSC sample carrier for all three steps, and the experimental temperature range. Differences in the weight matching of the samples and crucibles affects the heat capacity calculated using Equation 3. Sample placement in the DSC carrier across the three runs will change the $\Delta\varphi$ term and is taken

into account by using differences in the measured isothermal hold values. It has been observed that improper sample placement will lead to large differences in the heat flows of the isothermal holds; proper sample placement minimizes these differences. The calculated heat capacity from isothermal holds that differ >2 µV has been shown to differ by up to 0.5 J g^{-1} K^{-1} from values measured using the procedure described in this report. This is illustrated in Figure 17, which shows the results of FLiNaK heat capacity measurements performed using the same sample (S3) and sapphire reference on two separate days. In the measurement made on September 8th, the sapphire isothermal holds at 420 and 730 °C differed by 3.7 µV and the calculated heat capacity (Figure 17b) was ~2.03 J g^{-1} K^{-1}. The measurement made on September 10th using the same
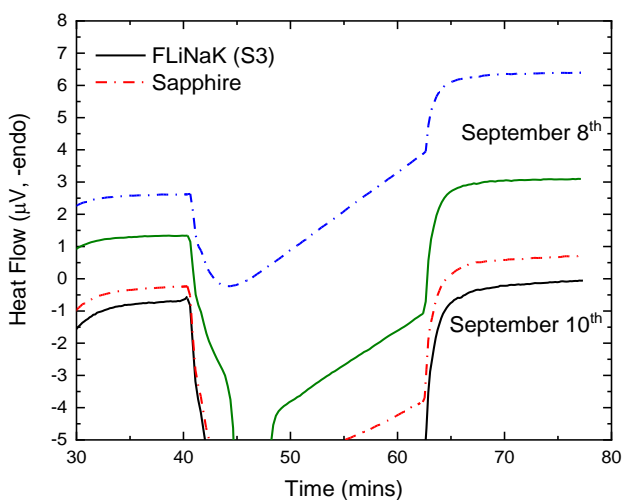
(a)
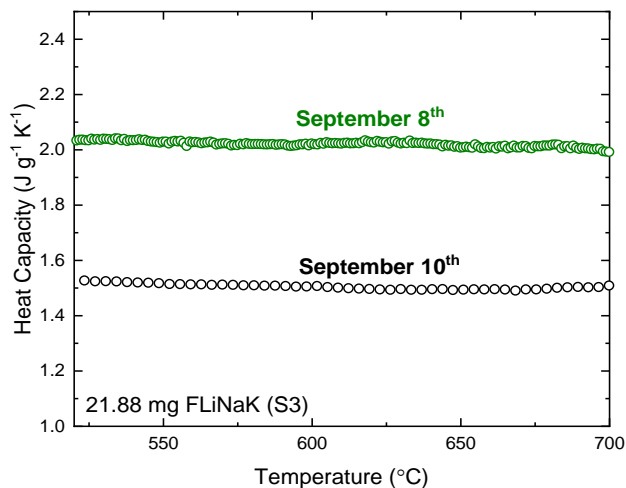
(b)

Figure 17. (a) Heat Flows for Sapphire and FLiNaK (S3) Measured on September 8th and September 10th and (b) Calculated Heat Capacity From Measurements on September 8th and September 10th.

sapphire reference had a difference of 0.8 µV and the calculated heat capacity was ~1.51 J g^{-1} K^{-1}. The greater instability of the instrument during the measurement made on September 8th is manifested as excessive variance in the background that affected the calculated heat capacity.

Finally, experimental temperature ranges of only 100–200 °C have been recommended to minimize changes in instrumental bias during the time required to make the three measurements using appropriate scan rates [5]. The temperature range of interest is greater than that and the additional correction included using the heat flows measured in isothermal holds at the low and high ends of the range increases the reliability of the measured values.

5.1. Heat Capacity of FLiNaK

Examination of the available literature for the measured salts indicates the method for heat capacity measurements developed at Argonne has reduced the uncertainty of measured heat capacities compared to results in the literature. The heat capacity of FLiNaK has been reported for measurements made by drop calorimetry and by DSC. The results of drop calorimetry performed at ORNL using an ice calorimeter exhibited unquantified but significant scatter leading the researchers to conclude that only a linear fit of the measured enthalpy data with respect to temperature was justified, meaning a the liquid-state heat capacity value was constant with temperature. They calculated the heat capacity of eutectic liquid FLiNaK to be 1.88 J g^{-1} K^{-1}, which was within 10% of other reported values using drop calorimetry across a multi-lab study [6].

DSC measurements with eutectic FLiNaK were performed by two groups utilizing different procedures. Rogers, Yoko, and Janz calibrated their DSC against the heats of fusion of five pure materials (In, Sn, Pb, KNO$_3$, LiCl-KCl) measured by drop calorimetry [7]. Calibrating the heat flow of the DSC by using heat of fusion is not recommended because the calibration is not guaranteed to be independent of temperature or the heating rate [8]. Rogers, Yoko and Janz utilized hermetically sealed gold DSC cells [9] to contain a small quantity of stoichiometric eutectic FLiNaK. The sample was conditioned by 14 consecutive heating-cooling cycles to ensure homogeneity then heated at 10 °C min^{-1} through the melting temperature. The heat capacity was calculated directly from the baseline-corrected heat flows of the sample. They determined the heat capacity of FLiNaK to range between 1.77–1.89 J g^{-1} K^{-1} at 477–587 °C with a reported repeatability within 2% [7]. Their work does not mention if isothermal measurements were used to check for deviations in heat flow and they do not mention the frequency of re-calibration of their heat flow.

The second lab using DSC, Khokhlov et al., used the same three-step procedure described in this report. They prepared FLiNaK in a similar manner described in this report but used Pt-Rh crucibles with perforated Pt-Rh lids. They performed 14 scans to precondition the FLiNaK the same as Rogers, Yoko, and Janz prior to heat capacity measurement. The heat flow of their liquid FLiNaK increased with each heating-cooling cycle from about 0.4 to 1 mW mg^{-1} for the first four reported

cycles, additional increases in heat flow were not shown or mentioned in their work. Their calculated heat capacity was 1.69–1.84 J g^{-1} K^{-1} at 477–587 °C with a reported variance of 5% [10]. They did not mention if their low and high isothermal holds differed and how that would affect their data. The FLiNaK results from Rogers et al. [7] and Khokhlov et al. [10] are shown overlaid with results for FLiNaK sample S3 that have (corrected) and have not (uncorrected) been adjusted for the isothermal background by using Equation 2 in Figure 18.
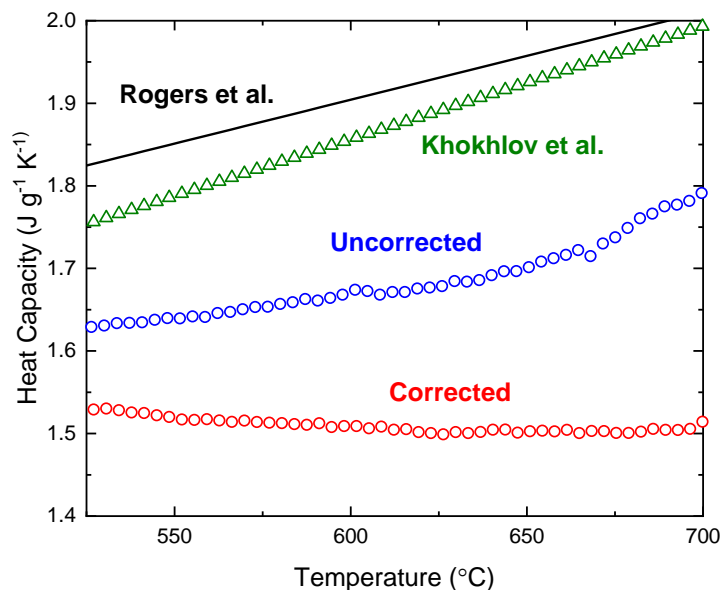

Figure 18. Overlay of the heat capacity of FLiNaK measured by Rogers et al., Khokhlov et al., an Uncorrected and Corrected Heat Capacity For FLiNaK S3.

The heat capacities determined by Rogers et al. [7] and Khokhlov et al. [10] are significantly higher than our measured values and increase with temperature. The results of Khokhlov et al. may be too high due to the increased heat flow they observed with repeated thermal cycling. Their use of perforated lids may have resulted in the loss of volatilized FLiNaK resulting in changes in the composition and unstable heat flows. Referring to Figure 8, the heat flow in our work remained stable during 11 heating-cooling cycles that confirms sample integrity was maintained by using hermetically sealed crucibles. It is important to note that the heat capacity measurements in our work and those by Khokhlov et al. were made relative to a sapphire standard and both are lower than those of Rogers et al. that determined by direct measurement without a sapphire reference. The higher values of Rogers et al. may be due to changes in conditions of their DSC after heat flow calibration. Note that our uncorrected heat capacity measurements with FLiNaK show the same upward trend as the results of both Rogers et al. and Khokhlov et al., but the temperature dependence is removed when results are corrected for effect of temperature on the heat flow quantified by using the isothermal holds. This suggests that neither Rogers et al. nor Khokhlov et

al. corrected the measured values for changes in heat flow with temperature during heat capacity determinations.

5.2. Heat Capacity of FLiBe

The heat capacity of FLiBe was calculated from drop calorimetry measurements using an ice calorimeter to be 2.323 J g^{-1} K^{-1} over the range 470–627 °C with reported uncertainties in the measurement larger than ± 3% due to corrections for impurities and off-composition samples [11]. More recent estimations of the heat capacity for FLiBe are 2.368 J g^{-1} K^{-1} with a reported accuracy of ± 20% [12]. Our results suggest the heat capacity of liquid FLiBe is about 1.84 J g^{-1} K^{-1}, which is consistent with the fixed value behavior reported in the literature [11]. The precision of the FLiBe heat capacity measurement is about 5% of the mean measured value, in line with expected precision of heat capacity measurements by DSC [5]. Our measurements of FLiBe show agreement within error of the literature values for the heat capacity of FLiBe.

6. Conclusions

Progress in making precise measurements of the heat capacity of molten FLiNaK and FLiBe has been demonstrated. The method described in this report is an adaptation of the ASTM standard to molten salt systems and has shown that Argonne method is capable of repeatable and precise measurements consistent with literature values. Appropriate experimental and data analysis has led to consistent results within 5% of the average measured value as demonstrated using two molten salt systems. This procedure can be directly applied to any molten salt and is easily implemented at other laboratories for quality and safety basis calculations. The data bases of measurements with eutectic FLiNaK and FLiBe support their use as reference materials to measure expected interlaboratory repeatability and interlaboratory reproducibility precisions for phase transition and heat capacity measurements.

Acknowledgements

References

[1]. M.A. Rose, E. Wu, T. Lichtenstein, and J. Krueger "Analytical Results for FLiNaK" Argonne National Laboratory, September 2020.

[2]. J.P.M. van der Meer, R.J.M. Konings, M.H.G. Jacobs, and H.A.J. Oonk "A Miscibility Gap in LiF-BeF_2 and LiF-BeF_2-ThF_4." *J. Nucl. Mats.*, 344, 2005, 94–99.

[3]. R.E. Thoma, H. Insley, H.A. Friedman, and G.M. Hebert. "Equilibrium Phase Diagram of the Lithium Fluoride-Beryllium Fluoride-Zirconium Fluoride System" *J. Nucl. Mats.* 27, 1968, 166–180.

[4]. ASTM E1269 "Specific Heat Capacity by Differential Scanning Calorimeter",<u>Annual Book of ASTM Standards,</u> Vol. 14.02. 2005.

[5]. G.W. Hohne, W.F. Hemminger and H.-J. Flammersheim. <u>Differential Scanning Calorimetry</u>. Second Edition. *Springer* 2003.

[6]. W.D. Powers and G.C. Blalock "Enthalpies and Heat Capacities of Solid and Molten Fluoride Mixtures" ORNL-1956, January 1956.

[7]. D.J. Rogers, T. Yoko, and G.J. Janz. "Fusion Properties and Heat Capacities of the Eutectic LiF-NaF-KF Melt" *J. Chem. Eng. Data.* 27, 1982, 366–367.

[8]. G. Della Gatta, M.J. Richardson, S.M. Sarge, and S. Stølen. "Standard, Calibration, and Guidelines in Microcalorimetry Part 2. Calibration Standards for Differential Scanning" *Pure and Appl. Chem.* 78, 7, 2006, 1455–1476.

[9]. G.J. Janz and G.N. Truong. "Melting and Premelting Properties of the KNO_3-$NaNO_2$-$NaNO_3$ Eutectic System" *J. Chem. Eng. Data.* 28, 1983, 201–202.

[10]. V. Khokhlov, I. Korzun, V. Dokutovich, E. Filatov. "Heat Capacity and Thermal Conductivity of Molten Ternary Lithium, Sodium, Potassium, and Zirconium Fluorides Mixtures." *J. Nucl. Maters.* 410, 2011, 32–38.

[11]. T.B. Douglas and W.H. Payne. "Measured Enthalpy and Derived Thermodynamic Properties of Solid and Liquid Lithium Tetrafluoroberyllate, Li_2BeF_4, from 273 to 900 K" *J. Res. Natl. Bur. Stands. A. Physics and Chemistry*. 73A, 5, 1969, 479–485.

[12]. D.F. Williams, "Assessment of candidate molten salt coolants for the NGNP/NHI Heat-Transfer Loop", Oak Ridge National Laboratory, ORNL/TM-2006/69, 2006.

Appendix A: Material Certificates for Salt Reagents

Figure A.1 Certificate of Analysis for LiF

Specification

1.05686.0050   Lithium fluoride 99.99 Suprapur®

	Specification	
Purity (metallic)	≥ 99.99	%
Ba (Barium)	≤ 5.0	ppm
Ca (Calcium)	≤ 2.0	ppm
Cd (Cadmium)	≤ 0.5	ppm
Co (Cobalt)	≤ 0.5	ppm
Cs (Cesium)	≤ 20	ppm
Cu (Copper)	≤ 0.5	ppm
Fe (Iron)	≤ 0.5	ppm
K (Potassium)	≤ 10	ppm
Mg (Magnesium)	≤ 0.5	ppm
Mn (Manganese)	≤ 0.5	ppm
Na (Sodium)	≤ 10	ppm
Ni (Nickel)	≤ 0.5	ppm
Pb (Lead)	≤ 0.5	ppm
Rb (Rubidium)	≤ 10	ppm
Sr (Strontium)	≤ 5	ppm
Zn (Zinc)	≤ 0.5	ppm

Evelyn Allmann
Responsible laboratory manager quality control

This document has been produced electronically and is valid without a signature.

Figure A.2 Certificate of analysis for NaF.

SIGMA-ALDRICH®

sigma-aldrich.com

3050 Spruce Street, Saint Louis, MO 63103, USA
Website: www.sigmaaldrich.com
Email USA: techserv@sial.com
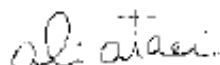Outside USA: eurtechserv@sial.com

Certificate of Analysis

Product Name:
Sodium fluoride – anhydrous, powder, 99.99% trace metals basis

Product Number:	450022
Batch Number:	MKBV9645V
Brand:	ALDRICH
CAS Number:	7681-49-4
MDL Number:	MFCD00003524
Formula:	FNa
Formula Weight:	41.99 g/mol
Quality Release Date:	17 JUL 2015

NaF

Test	Specification	Result
Appearance (Color)	White	White
Appearance (Form)	Powder	Powder
Gravimetric Analysis		45.3 %
% F With Lead Acetate		
ICP Major Analysis	Confirmed	Conforms
Confirms Sodium Component		
Purity	Meets Requirements	Meets Requirements
99.99% Based On Trace Metals Analysis		
Trace Metal Analysis	≤ 150.0 ppm	31.3 ppm
Aluminum (Al)		0.6 ppm
Barium (Ba)		0.5 ppm
Calcium (Ca)		1.5 ppm
Cesium (Cs)		5.0 ppm
Iron (Fe)		14.2 ppm
Potassium (K)		6.6 ppm
Lithium (Li)		0.9 ppm
Magnesium (Mg)		1.3 ppm
Manganese (Mn)		0.3 ppm
Rubidium (Rb)		0.4 ppm
Strontium (Sr)		< 0.1 ppm

Ali Ataei, Manager

Figure A.3 Certificate of analysis for KF.

SIGMA-ALDRICH®

Certificate of Analysis

Product Name:
Potassium fluoride – anhydrous, powder, ≥99.9% trace metals basis

Product Number:	449148	
Batch Number:	MKBX2566V	
Brand:	ALDRICH	
CAS Number:	7789-23-3	
MDL Number:	MFCD00011398	
Formula:	FK	
Formula Weight:	58.10 g/mol	
Quality Release Date:	31 DEC 2015	

KF

Test	Specification	Result
Appearance (Color)	White	White
Appearance (Form)	Powder	Powder
ICP Major Analysis Confirms K Component	Confirmed	Confirmed
Purity >=99.9% Based On Trace Metals Analysis	Conforms	Conforms
Trace Metal Analysis	$\leq$ 1000.0 ppm	614.7 ppm
Boron (B)		1.4 ppm
Calcium (Ca)		3.0 ppm
Chromium (Cr)		2.1 ppm
Cesium (Cs)		12.7 ppm
Iron (Fe)		8.4 ppm
Lithium (Li)		1.9 ppm
Manganese (Mn)		0.9 ppm
Sodium (Na)		527.4 ppm
Rubidium (Rb)		57.0 ppm

Michael Grady, Manager
Quality Control
Milwaukee, WI US

Figure A.4 Certificate of analysis for BeF₂.

MATERION
CERTIFICATE OF ANALYSIS

Customer: University of Chicago Argonne, LLC
Argonne National Laboratory
Building 46
9700 S. Cass Avenue
Lemont, IL 60439-4874

Date: 05/24/2019
Sales Order: 625877
P.O. 9A-64875

Specification: Be Fluoride

Material Description:

Item 10: 5.00 kg Be Fluoride

CHEMICAL COMPOSITION: (%)					MECHANICAL PROPERTIES						
Lot	19-05-01										
Be	19.2										
BeF₂	100										
Fe	<.01										
Al	<.02										
Na	.06										
Mn	<.002										
Cr	<.002										
Ni	<.004										

ADDITIONAL INFORMATION:

Materion testing for chemistry composition, mechanical and physical properties were tested at our laboratory in Elmore, OH or as necessary, outside laboratories under control of the Elmore Quality Department.
This material was inspected and tested and is conforming as required in accordance with the noted part, specification, drawing and revision. The test methods for these tests are available for review by the buyer.
This is to certify that during the manufacturing, process, examination, testing and packaging, our products do not come in contact with mercury or any of its compounds nor with any mercury-containing devices employing a single boundary or containment.

MATERION BRUSH INC.
QUALITY CONTROL

QA96-181-0

Chemical and Fuel Cycle Technologies Division

Argonne National Laboratory
9700 South Cass Avenue, Bldg. 205

Lemont, IL 60439

www.anl.gov